RSC Advances

PAPER

View Article Online
View Journal | View Issue

Cite this: *RSC Adv.*, 2024, **14**, 31251

Functionalized montmorillonite/epoxy resin nanocomposites with enhanced thermal and mechanical properties

Linna Su, * Changfa Fang and Huanzhong Luo

The poor interaction between the hydrophilic montmorillonite and hydrophobic epoxy resins leads to agglomeration of montmorillonite within epoxy resins, which finally results in poor macro properties of the epoxy resin nanocomposites. Although silane modification can improve the hydrophobicity of montmorillonite surface, the hydrolysis and condensation of silane lead to locking effect in the interlayer structure of functionalized montmorillonite. The effect of the functionalized montmorillonite on the properties of the epoxy resin remains unclear. Herein, we present multi technique approach to thoroughly evaluate the macro properties of the montmorillonite/epoxy resin nanocomposites, including dynamic mechanical thermal, thermo-mechanical, dielectric, water absorption and subsequently evaluate the molecular factors governing these characteristics. Importantly, the storage modulus has been enhanced by 44%, from 2416 MPa for pure epoxy resin to 2416 MPa for nanocomposites with 5.0 wt% functionalized montmorillonite. Our analysis reveals the increase of thermal stability and glass-transition temperature, as well as a reduction of the coefficient of thermal expansion with the addition of functionalized montmorillonite. Additionally, functionalized montmorillonite leads to decreased water absorption. This research aims to offer guidance for the development of high-performance montmorillonite/polymer nanocomposites, potentially opening up new applications for montmorillonite in polymer nanocomposites.

Received 27th April 2024
Accepted 23rd September 2024

DOI: 10.1039/d4ra03125c

rsc.li/rsc-advances

Introduction

Polymer nanocomposites incorporating nanoscale inorganic fillers have garnered significant attention due to their superior overall properties, including thermal, mechanical, electrical, and electromagnetic performance compared to pure polymers.[1] Among various inorganic fillers, montmorillonite is one of the most widely chosen fillers,[2,3] mainly due to its high specific surface area and rich cations between the layers of the montmorillonite crystal structure.[4] Improving the compatibility between hydrophilic montmorillonite surface and hydrophobic polymer is crucial to prevent agglomeration of montmorillonite within the polymer matrix. Therefore, it is desirable to modify montmorillonite with organic groups for better affinity with polymers.

In general, the modification of montmorillonite surfaces has generally been approached through two primary methods: physical and chemical.[5] The compatibility of hydrophobic polymers with montmorillonite can be effectively enhanced by employing various surfactants, which is a commonly adopted physical approach for modification.[6,7] However, physical modification does not establish an effective connection between the montmorillonite and polymer matrix. Additionally, a majority of surfactants exhibit instability when subjected to the typical processing temperature of polymers.[8] The potential presence of a weak electrostatic interaction may give rise to the formation of a distinct interface between hydrophilic montmorillonite and polymers, which could adversely impact the mechanical properties of polymer nanocomposites.[9] The silane grafting of hydrophobic groups to the montmorillonite surfaces has been attracted great attention.[10–12] The organic groups commonly used for better affinity with polymers include amino, epoxy, methacrylic groups, *etc.* The formation of a covalent bond enables the enduring immobilization of the organic components,[13] which results in uniform dispersion of montmorillonite in polymer matrix.[14] For example, V. Nigam and co-workers reported an epoxy resin/functionalized montmorillonite nanocomposite with enhanced mechanical properties.[15] However, the thermal stability of the functionalized montmorillonite filled nanocomposites is less than that of raw montmorillonite filled nanocomposites, probably due to the presence of organic species (octadecylammonium ions), which is less thermally stable than inorganic species. In our previous study,[16] montmorillonite was silylated with 3-aminopropyltriethoxysilane, and a phenomenon of locking effect was observed during the silylation process. However, the effect of the silylated montmorillonite on the properties of the polymers

Shenzhen Polytechnic University, Shenzhen 518055, China

remain unclear. The lack of a reliable and user-friendly experimental method for investigating the correlation between functionalized montmorillonite and macroscopic characteristics poses a significant challenge, hindering the systematic development of montmorillonite/polymer composites with targeted attributes.

In this study, we introduce a methodology to assess the macroscopic characteristics of functionalized montmorillonite/epoxy resin nanocomposites. We investigated their dynamic mechanical thermal behavior, thermo-mechanical properties, dielectric performance, water absorption capacity, and subsequently examining the molecular factors that govern these properties. Epoxy resins were selected as model polymer matrix, due to their fascinating properties such as strong adhesion, good chemical stability, high mechanical strength, and ease of processing and shaping. We expect that the amino group of functionalized montmorillonite attacks the epoxide ring of epoxy resin covalently, and thus improves the interfacial interactions between montmorillonite and epoxy resins, which is consistent with previous studies.[17–20] Our analysis unambiguously reveals the increase of thermal stability and glass-transition temperature with the addition of functionalized montmorillonite. The addition of montmorillonite also results in a reduction of the coefficient of thermal expansion, while decreasing water absorption. This study aims to offer insights for creating high-performance montmorillonite/polymer nanocomposites and exploring new applications for montmorillonite in polymer nanocomposites.

Experimental

Materials

A monomer of epoxy resin, 3,4-epoxycyclohexylmethyl-3,4-epoxy-cyclo-hexane carboxylate (ERL 4221) manufactured by Tetrachem in China, was employed. This particular epoxy resin monomer possesses an epoxy equivalent mass measuring 127.0 g mol^{-1}. The curing agent employed was methylhexahydrophthalic anhydride (MHHPA) sourced from Bangcheng Co. Ltd, China, with a minimum purity of 98%. 2-Ethyl-4-methylimidazole (EMI) as curing promoter, was obtained from the same supplier with a purity level of at least 99%. Montmorillonite (Mt) used in the experiment was acquired from Neimeng, China. The montmorillonite utilized in this study was obtained from the supplier after undergoing a purification process to eliminate impure minerals, with the exception of quarts. No further treatment was conducted on the received montmorillonite. The chemical formula of the Mt is $Na_{0.2}Ca_{0.1}Al_2Si_4O_{10}(OH)_2(H_2O)_{10}$, with the molecular weight of 549.07 g mol^{-1}. The 3-aminopropyltriethoxysilane (APTES) used in this research was procured from Aldrich (≥98%) and employed without any additional modifications.

Functionalization of montmorillonite

In a typical experiment, a dispersion of Mt (10.0 g) in cyclohexane (200 mL) was prepared and subjected to stirring, and then sonicated. Afterwards, while maintaining constant agitation, a gradual addition of APTES (8.0 g) was incorporated into the dispersion. Subsequently, the resulting blend underwent stirring for a period of 10 hours at a temperature set to 80 °C. To eliminate any excess silane present, the reaction product underwent centrifugation followed by washing with cyclohexane. After being dried for a period of 24 hours at 80 °C, the collected powders were identified as functionalized montmorillonite, designated as MtS.

Preparation of the montmorillonite/epoxy resin nanocomposites

The solvent-free method was utilized to prepare nanocomposites of montmorillonite/epoxy resin with varying amounts of MtS. In accordance with standard procedures, equivalent quantities of ERL 4221, MHHPA, EMI, and MtS were homogeneously blended using a high-speed mixer under vacuum conditions (Speedmixer, DAC 1200-300). Subsequently, the resultant mixture was carefully poured into a mold and underwent curing at a temperature of 140 °C for two hours before being further heated at 220 °C for an additional two hours. The concentrations of MtS in the ensuing nanocomposites were adjusted to be 3 wt%, 5 wt%, and 10 wt% respectively. These specific compositions were denoted as follows: MtS-3/EP, MtS-5/EP, and MtS-10/EP. To enable comparative analysis, pure epoxy and montmorillonite/epoxy resin nanocomposite with 5 wt% Mt loading (Mt-5/EP) were also prepared following the same procedure.

Characterization

The fracture morphology of the MtS/EP nanocomposites was obtained by scanning electron microscopy (SEM, ZEISS GeminiSEM 300) at a high voltage of 10 kV, according to ASTM E986-04(2017) standard. The TA Q600 thermobalance from TA Instruments was utilized to conduct the thermogravimetric analysis, according to ASTM E1131 standard, with a nitrogen flow rate of 100 mL min^{-1}. The temperature was increased from 30 to 800 °C at a rate of 5 °C min^{-1} during the heating process. Dynamic mechanical thermal analysis was conducted with a dynamic mechanical thermal analyzer (DMA, Q800, TA Instrument), according to ASTM D4065 standard, with the heating rate of 3 °C min^{-1} at 1.0 Hz, and temperature ranging from 25 to 300 °C. The specimens had dimensions measuring 6 mm × 2 mm × 30 mm. To determine the glass transition temperature (T_g), we identified it as the temperature corresponding to the peak value on the tan δ curve. To determine the dielectric properties at ambient temperature, an impedance analyzer (Agilent 4294A) was used across frequencies ranging from 100 Hz to 10 MHz. Prior to testing, silver paste was applied onto the samples, according to ASTM D150 standard. The coefficient of thermal expansion (CTE) for the MtS/EP nanocomposites was determined using a Thermomechanical Analyzers (TMA/SDTA 2+, Mettler Toledo Instruments), according to ASTM E831 standard. A 0.02 N force was exerted during the heating process, with a temperature increase rate of 5 °C min^{-1} from room temperature to 300 °C in the presence of

nitrogen gas. The equation provided below was used to calculate the values of CTE:

$$\mathrm{CTE} = \frac{\mathrm{d}L}{\mathrm{d}T} \times \frac{1}{L_0} \quad (1)$$

where the slope of the length–temperature curve for the material, denoted as $\mathrm{d}L/\mathrm{d}T$, represents how the length changes with temperature. L_0 refers to the initial length measured at 25 °C. On the basis of ASTM D570 standard, the weighing method was employed to determine the water absorption (WA) of the nanocomposites consisting of MtS/EP. Initially, the specimens measuring 20 mm × 20 mm × 2 mm were placed in an oven set at 80 °C for 24 hours and subsequently weighed. Subsequently, the specimens were submerged in distilled water at 25 °C. After 24 hours, the specimens were removed from the water and dried with absorbent paper to eliminate any surface moisture before being reweighed. The WA values of the specimens were determined by means of the subsequent formula:

$$\mathrm{WA} = \frac{W_1 - W_0}{W_0} \times 100\% \quad (2)$$

where W_0 and W_1 represented the weight of dry substance and the materials post water absorption, correspondingly.

Results and discussion

Characterization of the functionalized montmorillonite

Fig. 1 shows the Fourier transform infrared spectroscopy of the MtS. Compared to the raw Mt, the functionalized Mt (MtS) demonstrates a distinct vibration at 2934 cm^{-1} corresponding to the antisymmetric stretching of $–CH_2$, along with an out-of-plane deformation of –CH observed at 696 cm^{-1}. Two new peaks at 3315 cm^{-1} and 1520 cm^{-1} are attributed to antisymmetric stretching of N–H bond and C–N bond, respectively, which indicate existence of APTES in the MtS. In addition, the intensity of the –OH stretching vibration at 3620 cm^{-1} and Al–OH bending vibration at 916 cm^{-1} decreases after silane functionalization. These observations suggested the successful grafting of silane onto montmorillonite surface as accompanied by the consumption of hydroxyl groups. In the FTIR spectra of unadulterated Mt and MtS, the stretching vibration of Si–O–Si can be identified by observing a peak at approximately 1032 cm^{-1} along with a secondary peak around 1085 cm^{-1}. The successful silane functionalization by APTES, a silane coupling agent, is indicated by a slight shift in the vibration frequency from 1032 cm^{-1} (raw Mt) to about 1037 cm^{-1} (MtS), as well as a subtle reduction in intensity observed for the shoulder.

Thermogravimetric analysis was conducted to determine the amounts of APTES grafting. The results showed that the mass loss below 200 °C was due to absorbed –OH groups, while the mass loss between 200 and 600 °C resulted from APTES evaporation and/or decomposition. Following silane modification, dehydroxylation-related mass loss significantly decreased, likely due to hydroxyl group consumption during silylation reaction. Notably, the mass loss at 200 °C indicated physically adsorbed APTES on Mt surfaces, whereas those at 330 °C and 426 °C were attributed to covalently bonded APTES at broken edges or adsorbed/intercalated in interlayer spaces on Mt surfaces.[21–23] The thermal degradation of APTES occurs at approximately 540 °C, leading to a reduction in mass. The dehydroxylation process of the aluminosilicate groups present in the pristine Mt clay structure results in a mass loss observed at 637 °C.[24] In comparison to the raw Mt at 700 °C, we have determined that the APTES grafting content is approximately 5.30 wt% (Fig. 2).

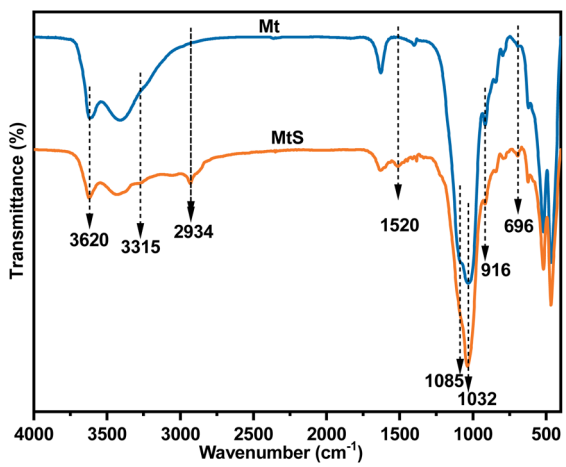

Fig. 1 FTIR spectra of the pristine and functionalized montmorillonite.

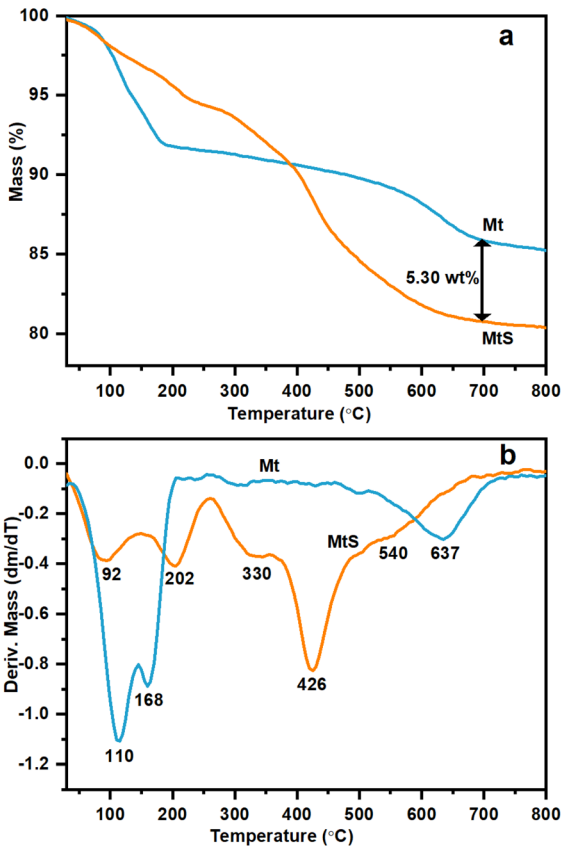

Fig. 2 Thermogravimetric analysis (a) and differential thermogravimetric (b) curves of the pristine and functionalized montmorillonite.

Microstructure

Fig. 3 shows the SEM images of fracture surface of the MtS/EP nanocomposite with 5 wt% MtS. Compared with Mt/EP nanocomposite (Fig. 3a), the aggregation of montmorillonite is less obvious (Fig. 3b), indicating an enhanced interfacial interaction between montmorillonite and epoxy resins.

Thermal stability

Fig. 4 shows thermogravimetric analysis (TGA) curves of the MtS/EP nanocomposites. As the temperature increases, the TGA curves of MtS/EP nanocomposites shows a sharp decline, indicating degradation. Above 400 °C, there is a significant decrease in mass loss rate for each system, suggesting that most groups within the epoxy resin structure have undergone thermal decomposition. The temperature at which 5% mass loss, defined as $T_{5\%}$, is used as signature of thermal stability. As shown in Table 1, the $T_{5\%}$ of the pure epoxy resins is at 343 °C. Upon incorporating montmorillonite, both Mt-5/EP and MtS-5/EP showed reduced $T_{5\%}$ values of 328 °C and 339 °C respectively. This decrease may be ascribed to a decline in the density of cross-linking within the epoxy resins after montmorillonite addition. Interestingly, the $T_{5\%}$ value of MtS-5/EP is much higher than that of the Mt-5/EP, indicating that the functionalization is benefit to thermal stability. This is likely due to enhanced compatibility of functionalized montmorillonite with epoxy resins. Furthermore, the presence of montmorillonite residues in the Mt/EP nanocomposites resulted in higher char yields at approximately 500 °C compared to those observed for pure epoxy.

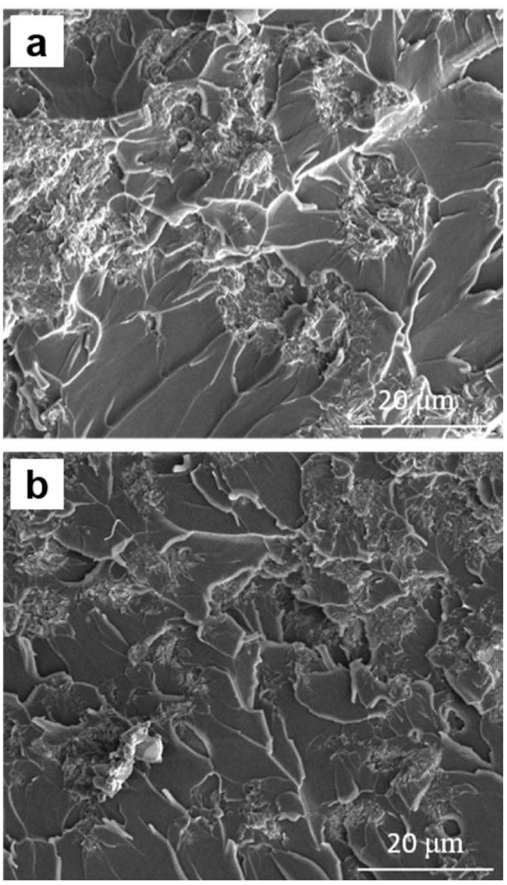

Fig. 3 SEM images of cross-sections of (a) Mt-5/EP, and (b) MtS-5/EP.

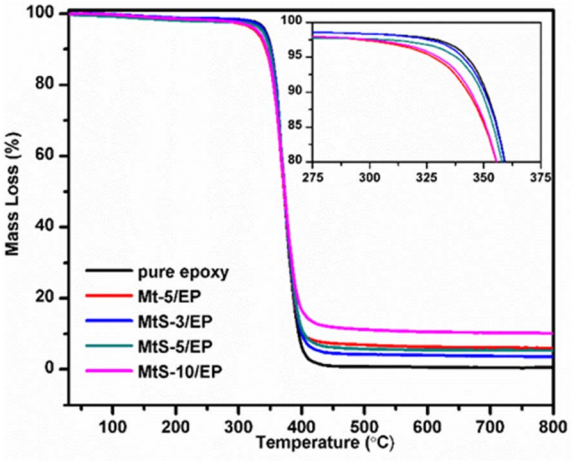

Fig. 4 Thermogravimetric analysis curves of the pure epoxy, Mt-5/EP, MtS/EP nanocomposites with various MtS contents.

Table 1 Temperature $T_{5\%}$, storage modulus, and T_g for pure epoxy, Mt-5/EP, MtS/EP nanocomposites with various MtS contents

Samples	$T_{5\%}$ (°C)	Storage modulus (30 °C, MPa)	T_g (°C)
Pure epoxy	343	1674	223
MtS-3/EP	341	2228	230
MtS-5/EP	339	2416	226
MtS-10/EP	331	2245	224
Mt-5/EP	328	1884	229

Dynamic mechanical properties

DMA is a useful technique for assessing the physical and chemical properties of polymer based nanocomposites, offers valuable information on their toughness and molecular relaxation through parameters such as storage modulus (G'), loss modulus (G''), and tan δ (G''/G').[25] The DMA curves of the nanocomposites consisting of MtS and epoxy resin are displayed in Fig. 5. Table 1 summarizes the relative variations in G' for the MtS/EP nanocomposites at a temperature of 30 °C. The addition of MtS results in an improvement in G', from 1674 MPa for pure epoxy resin to 2416 MPa for the MtS-5/EP at a temperature of 30 °C. The enhancement of the G' is ascribed to the strengthening impact exerted by MtS on the epoxy resin, as it restricts the movement of polymer chains within epoxy resin and enhances stress transmission under applied loads.[26] In addition, the incorporation of MtS into epoxy resins results in higher G' values compared to Mt/EP nanocomposites. This can be attributed to the improved interfacial interaction between MtS and epoxy resins, which enhances the immobilization of epoxy resin chains and provides more load transfer centers. The loss modulus and tan δ curves for MtS/EP nanocomposites

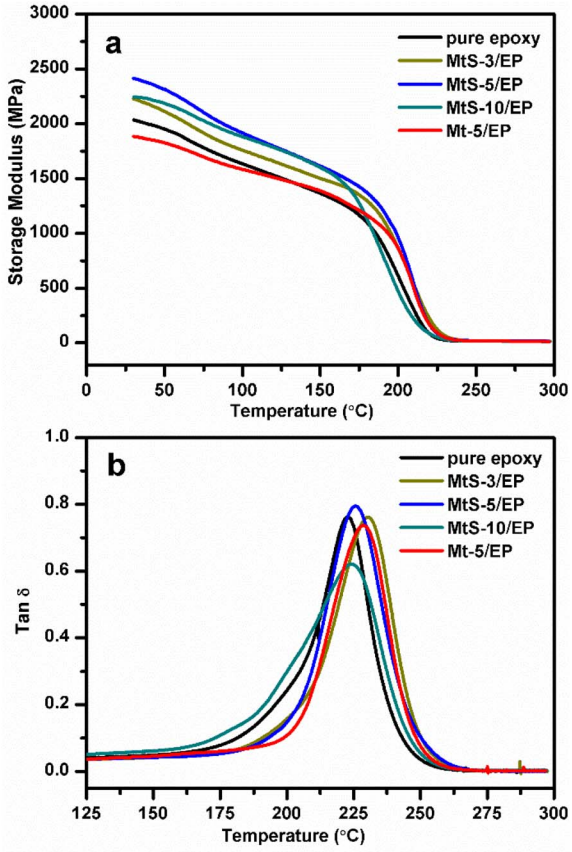

Fig. 5 Storage modulus (a) and tan δ (b) of pure epoxy, Mt-5/EP, MtS/EP nanocomposites with various MtS contents as a function of temperature.

exhibit the presence of a transition peak, indicates that there is no phase separation between clay and epoxy. Glass transition temperature (T_g), an important property of epoxy resins, reflects changes in polymer chain dynamics and thermal stability. T_g is defined as the temperature at which the maximum peak occurs in either the loss modulus or tan δ (Fig. 5b). As shown in Table 1, incorporating MtS leads to a higher T_g compared to pure epoxy. With 3 wt% MtS, the maximum T_g value reaches 230 °C, which is approximately 7 °C higher than that of pure epoxy (223 °C). This is attributed to enhanced interactions between MtS and the epoxy network, resulting in restricted chain mobility. However, further increasing MtS content slightly decreases T_g due to potential aggregation of MtS particles.

Coefficient of thermal expansion

The coefficient of thermal expansion (CTE) is a significant concern in the use of polymers for engineering purposes, as materials with low CTE are better able to maintain dimensional stability. In order to evaluate how MtS affects the thermal dimensional stability of epoxy resins, we utilized TMA (as shown in Fig. 6). The temperature-dependent length curves for all samples showed a gradual transition from a glassy state to a rubbery state. CTE values were determined for the montmorillonite/epoxy resin nanocomposites by analyzing the slope of thermal expansion curves below and above T_g within

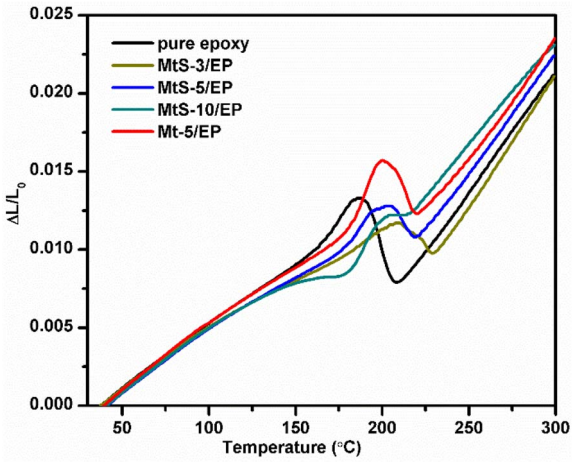

Fig. 6 TMA curves of the pure epoxy, Mt-5/EP, MtS/EP nanocomposites with various MtS contents.

Table 2 CTE and T_g values of pure epoxy, Mt-5/EP, MtS/EP nanocomposites with various MtS contents

Composites	CTE (10^{-6} °C^{-1})	T_g (°C)
Pure epoxy	80.0	199
MtS-3/EP	61.4	226
MtS-5/EP	71.1	212
MtS-10/EP	74.0	209
Mt-5/EP	76.1	214

temperature ranges of 40–150 °C (Table 2). The CTE of pure epoxy resin was 80.0 × 10^{-6} °C^{-1}, but the CTE of the nanocomposites decreased with the addition of montmorillonite. This was because rigid montmorillonite has good dimensional stability and do not expand when heated in the epoxy resin system. When the MtS content was 3%, the CTE was 61.4 × 10^{-6} °C^{-1}. Further increasing MtS resulting in slight increase of the CTE. The CTE of nanocomposite was not only related to the rigidity of montmorillonite, but also to the degree of dispersion of montmorillonite. The good dispersibility of MtS can effectively combine with the epoxy resin, reducing the CTE of nanocomposites. However, the higher content of MtS leads to uneven dispersion in the system, which can easily cause local aggregation or precipitation, and the inhibitory effect on the expansion of epoxy resin is not significant. Furthermore, at an equivalent filler loading level (5 wt%), it was found that MtS/EP nanocomposites demonstrated even lower CTE compared to Mt/EP, suggesting that functionalization had beneficial effects on enhancing interfacial strength between MtS and epoxy resin. The T_g values of epoxy resin and its composite materials are lower than those measured by DMA method (Table 1), but the trend of change is consistent with the test results of DMA, which verifies the test results of DMA.

Dielectric properties

Dielectric properties, such as dielectric constant and dielectric loss, play a crucial role in polymer nanocomposites. The

dielectric constant indicates the capacity to store electric charges within an electric field, while the dissipation of energy caused by the flow of conductive carriers in response to alternating electric fields is indicated by the dielectric loss. As depicted in Fig. 7, the frequency-dependent decrease in the dielectric constant of MtS/EP nanocomposites can be attributed to interfacial relaxation. Incorporating MtS into the composites leads to an increase in dielectric constant compared to pure epoxy resins (Fig. 7a), primarily due to MtS having a higher dielectric constant than pure epoxy resin. Interestingly, unlike other thermal properties, functionalizing Mt does not alter the dielectric constant of Mt/EP nanocomposites. On another note, with increasing frequency (Fig. 7b), there is an observed rise in the dielectric loss of the MtS/EP nanocomposites because rotational motions of dipolar groups fail to keep pace with changes in electric field frequency. However, upon adding MtS content and implementing surface modification techniques, there is only a slight increase in the overall dielectric loss for these composites. It is worth mentioning that even at higher frequencies, where further increases are seen in the dielectric loss values (<0.05), this material still exhibits potential applications within electronic information industries. Recently, interfacial information between polymer and fillers has been found to exhibit retarded dynamics by dielectric spectroscopy,[27,28] showing an individual interfacial relaxation (α_{int}) with suppressed cooperativity, as compared to the main α relaxation (bulk-like polymer). However, in our system, there is no obvious additional peak of interfacial relaxation, probably due to a strong Maxwell–Wagner–Sillars polarization and a high dc conductivity overlap with the interfacial layer contribution to the dielectric spectra.[29]

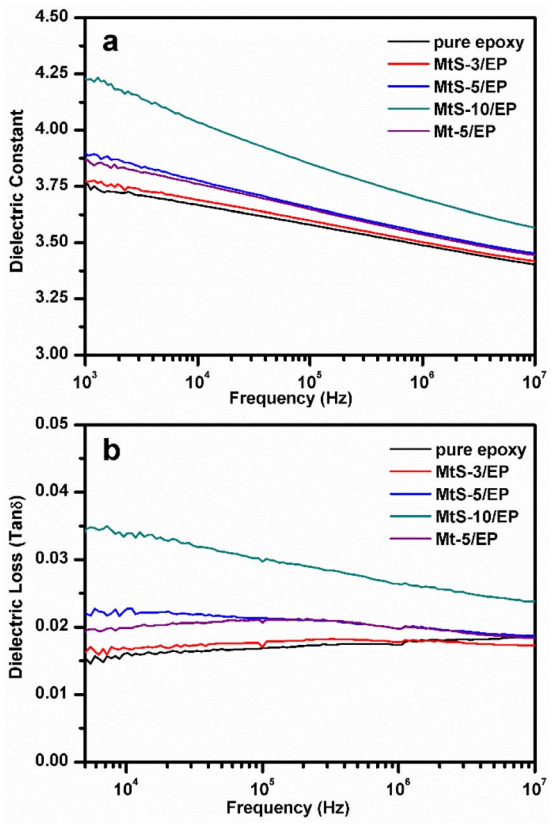

Fig. 7 The dielectric properties of pure epoxy, Mt/EP, MtS/EP nanocomposites with various MtS contents, including the (a) dielectric constant and (b) dielectric loss.

Water absorption

Refraining from the absorption of water by polymer nanocomposites is crucial in order to maintain their long-term property. Hence, it is imperative to minimize the water uptake of these materials. The impact of MtS on the water absorption behavior of MtS/EP nanocomposites was investigated. As shown in Fig. 8, the water absorption for the pure epoxy resin increases with prolonged immersion time, eventually reaching 2.4 wt% after being immersed for 168 hours. When the experiment time above 168 h, the change of moisture absorption is small and up to saturation. In contrast, for the MtS/EP nanocomposites, although there was also an increase in water absorptions with longer immersion times, they remained lower compared to those observed in the pure epoxy resin. The penetration of water molecules through the epoxy network could be attributed to the occurrence of water absorption. The pure epoxy resin tends to allow water molecules to enter the defects or voids, when it is permeated with saturated moisture before being evenly distributed throughout. The presence of MtS enhances polymerization, resulting in a more intricate pathway for water penetration. This is because the clay platelets prevent water molecules from penetrating, thereby improving the resistance to water. Furthermore, MtS/EP exhibits slightly lower water absorption compared to Mt/EP, indicating that MtS contributes positively towards preventing water infiltration. This phenomenon can be attributed to the incorporation of silane groups onto the surface of Mt, which impede accessibility to specific locations and effectively diminish the volume of micro-voids. There is no quantitative relationship between moisture

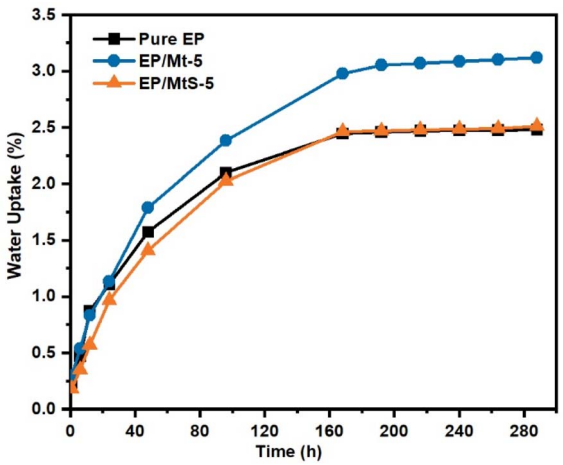

Fig. 8 Water absorption behavior of pure epoxy and Mt/EP nanocomposites.

absorption and other physical properties, such as dielectric, mechanical, and thermal properties. High moisture absorption usually leads to deteriorating physical properties.

Conclusions

In conclusion, we have comprehensively characterized the macro properties of the functionalized montmorillonite/epoxy resin nanocomposites, including dynamic mechanical thermal, thermo-mechanical, dielectric, water absorption and then analyzing molecular parameters controlling these properties. FTIR and TGA suggest the successful silane functionalization by silane coupling agent, with the grafting content of APTES about 7.7 wt%. The functionalized montmorillonite/epoxy resin shows more thermal stability than the montmorillonite filled epoxy resin nanocomposite, as evidenced by a higher onset temperature for thermal decomposition. This indicates that the functionalization process has a positive effect on enhancing thermal stability. The storage modulus has been enhanced by 44%, from 2416 MPa for pure epoxy resin to 2416 MPa for nanocomposites with 5.0 wt% functionalized montmorillonite. Additionally, the increased intercalation and interfacial interaction between montmorillonite and epoxy resins lead to an increased glass transition temperature when compared to the montmorillonite/epoxy resin. Our analysis also indicates that the coefficient of thermal expansion and water absorption decreased with the addition of functionalized montmorillonite. This study aims to offer valuable insights for constructing high-performance montmorillonite/polymer nanocomposites. Such functionalized montmorillonite/epoxy resin nanocomposites may attract attention to industrial sectors for structural, automotive, and packaging applications. We also envision that this approach can expand to other polymers with more complex chemical groups.

Data availability

The authors confirm that the data supporting the findings of this study are available within the article.

Author contributions

S. L. Su: conceptualization, methodology, project administration, funding acquisition, data curation, writing—original draft preparation, writing—review and editing; C. F. Fang: validation, supervision; H. Z. Luo: software, investigation.

Conflicts of interest

There are no conflicts to declare.

Acknowledgements

This work was financially supported by the Foundation of Shenzhen Polytechnic University (No. 6017-22 K210169991).

Notes and references

1 M. R. Begley, D. S. Gianola and T. R. Ray, *Science*, 2019, **364**(6447), eaav4299.
2 Y. Zhang, D. Xu, L. Yuan, Q. Gao, Q. Yu, J. Chen, Y. Cheng, A. Sun, G. Xu and J. Guo, *Mater. Today Commun.*, 2023, **37**, 107208.
3 I. Spiridon, A. Bele, I. Apostol, M. V. Dinu and N. Anghel, *J. Polym. Environ.*, 2024, **32**, 2014–2030.
4 Y. Zare and K. Y. Rhee, *Appl. Clay Sci.*, 2017, **150**, 42–46.
5 H. He, Q. Tao, J. Zhu, P. Yuan, W. Shen and S. Yang, *Appl. Clay Sci.*, 2013, **71**, 15–20.
6 H. Zhang, M. Xia, F. Wang, P. Li and M. Shi, *Appl. Clay Sci.*, 2021, **207**, 106086.
7 E. Mahdavi, M. Haghighi-Yazdi, M. M. Mashhadi and R. Khaledialidusti, *J. Appl. Polym. Sci.*, 2020, **138**, 49471.
8 J. Madejová, Ľ. Jankovič, M. Slaný and V. Hronský, *Appl. Surf. Sci.*, 2020, **503**, 144125.
9 M. Huskić, M. Žigon and M. Ivanković, *Appl. Clay Sci.*, 2013, **85**, 109–115.
10 L. M. Dongmo, S. L. Z. Jiokeng, C. N. Pecheu, A. Walcarius and I. K. Tonle, *Appl. Clay Sci.*, 2020, **191**, 105602.
11 A. Gil, L. Santamaría, S. A. Korili, M. A. Vicente, L. V. Barbosa, S. D. de Souza, L. Marçal, E. H. de Faria and K. J. Ciuffi, *J. Environ. Chem. Eng.*, 2021, **9**, 105808.
12 M. Asgari and U. Sundararaj, *Appl. Clay Sci.*, 2018, **153**, 228–238.
13 N. Takahashi and K. Kuroda, *J. Mater. Chem.*, 2011, **21**, 14336–14353.
14 M. Sandomierski, Z. Buchwald and A. Voelkel, *Appl. Clay Sci.*, 2020, **198**, 105822.
15 V. Nigam, D. K. Setua, G. N. Mathur and K. K. Kar, *J. Appl. Polym. Sci.*, 2004, **93**, 2201–2210.
16 S. N. Danilova, A. N. Ivanov, A. M. Spiridonov, E. V. Abakunova and A. A. Okhlopkova, *Mater. Today Commun.*, 2023, **37**, 107408.
17 L. Su, Q. Tao, H. He, J. Zhu and P. Yuan, *Mater. Chem. Phys.*, 2012, **136**(2), 292–295.
18 M. W. Sabaa, M. Abdelhakim and S. M. A. Soliman, *Bull. Mater. Sci.*, 2020, **43**, 126.
19 M. Işık and G. Ahmetli, *Ind. Crops Prod.*, 2024, **221**(1), 119421.
20 J. Y. Qin, W. C. Zhang and R. J. Yang, *Mater. Des.*, 2019, **178**(15), 107834.
21 J. Chrusciel and E. Lesniak, *Prog. Polym. Sci.*, 2015, **41**, 67–121.
22 H. He, J. Duchet, J. Galy and J.-F. Gerard, *J. Colloid Interface Sci.*, 2005, **288**, 171–176.
23 A. M. Shanmugharaj, K. Y. Rhee and S. H. Ryu, *J. Colloid Interface Sci.*, 2006, **298**, 854–859.
24 L. Su, Q. Tao, H. He, J. Zhu, P. Yuan and R. Zhu, *J. Colloid Interface Sci.*, 2013, **391**, 16–20.
25 F. Piscitelli, P. Posocco, R. Toth, M. Fermeglia, S. Pricl, G. Mensitieri and M. Lavorgna, *J. Colloid Interface Sci.*, 2010, **351**, 108–115.
26 J. M. González-Domínguez, A. Ansón-Casaos, A. M. Díez-Pascual, B. Ashrafi, M. Naffakh, D. Backman, H. Stadler,

A. Johnston, M. Gómez and M. T. Martínez, *ACS Appl. Mater. Interfaces*, 2011, **3**, 1441–1450.
27 G. Šebenik, M. Huskić, D. Vengust and M. Žigon, *Appl. Clay Sci.*, 2015, **109–110**, 143–150.
28 P. A. Klonos, O. V. Goncharuk, E. M. Pakhlov, *et al.*, *Macromolecules*, 2019, **52**, 2863–2877.
29 S. Wang, Z. Luo, J. Liang, *et al.*, *ACS Nano*, 2022, **16**, 13612–13656.